HHS Public Access

Author manuscript

Bone. Author manuscript; available in PMC 2022 March 01.

Published in final edited form as:

Bone. 2021 March ; 144: 115825. doi:10.1016/j.bone.2020.115825.

Electrical Stimulation of Hindlimb Skeletal Muscle has Beneficial Effects on Sublesional Bone in a Rat Model of Spinal Cord Injury

Wei Zhao[1,2], **Yuanzhen Peng**[1], **Yizhong Hu**[4], **X. Edward Guo**[4], **Jiliang Li**[5], **Jay Cao**[6], **Jiangping Pan**[1], **Jian Q. Feng**[7], **Christopher Cardozo**[1,2,3], **Jonathan Jarvis**[8], **William A. Bauman**[1,2,3], **Weiping Qin**[1,2,*]

[1]National Center for the Medical Consequences of SCI, James J. Peters VA Medical Center, Bronx, NY;

[2]Departments of Medicine, Icahn School of Medicine at Mount Sinai, New York, NY;

[3]Rehabilitation Medicine, Icahn School of Medicine at Mount Sinai, New York, NY;

[4]Department of Biomedical Engineering, Columbia University, New York, NY;

[5]Indiana University Purdue University Indianapolis, Indianapolis, IN, USA;

[6]United States Department of Agriculture Agricultural Research Service Human Nutrition Research Center, Grand Forks, North Dakota;

[7]Baylor College of Dentistry, TX A&M, Dallas, TX, USA;

[8]School of Sport and Exercise Sciences, Liverpool John Moores University, Liverpool L3 3AF, United Kingdom.

Abstract

Spinal cord injury (SCI) results in marked atrophy of sublesional skeletal muscle and substantial loss of bone. In this study, the effects of prolonged electrical stimulation (ES) and /or testosterone enanthate (TE) on muscle mass and bone formation in a rat model of SCI were tested. Compared to sham-transected animals, a significant reduction of the mass of soleus, plantaris and extensor digitorum longus (EDL) muscles was observed in animals 6 weeks post-SCI. Notably, ES or ES +TE resulted in the increased mass of the EDL muscles. ES or ES+TE significantly decreased mRNA levels of muscle atrophy markers (e.g., MAFbx and MurF1) in the EDL. Significant decreases in bone mineral density (BMD) (−27%) and trabecular bone volume (−49.3%) at the

*Corresponding Author: Weiping Qin, MD, Ph.D., James J. Peters Veteran Affairs Medical Center, 130 West Kingsbridge Road, Bronx, NY 10468, USA, Tel: 718-584-9000 X1831, weiping.qin@mssm.edu or weiping.qin@va.gov.

Author Contributions

WQ and WZ were responsible for study design and data analysis. WZ, YP, YH, EG, JL, JC, JP, JQF, JJ and WAB provided consultation on and performed the experimental procedures to generate the data as well as data interpretation for the study. The manuscript was written by WQ, WZ, and CC and was revised and approved by all authors. WQ takes responsibility for the integrity of the data analysis.

Author Disclosure Statement.

No competing financial interests exist.

distal femur were observed in animals 6 weeks post injury. TE, ES and ES+TE treatment significantly increased BMD by +6.4%, +5.4%, +8.5% and bone volume by +22.2%, and +56.2% and+ 60.2%, respectively. Notably, ES alone or ES+TE resulted in almost complete restoration of cortical stiffness estimated by finite element analysis in SCI animals. Osteoblastogenesis was evaluated by colony-forming unit-fibroblastic (CFU-F) staining using bone marrow mesenchymal stem cells obtained from the femur. SCI decreased the CFU-F^+ cells by −56.8% compared to sham animals. TE or ES+TE treatment after SCI increased osteoblastogenesis by +74.6% and +67.2%, respectively. An osteoclastogenesis assay revealed significantly increased $TRAP^+$ multinucleated cells (+34.8%) in SCI animals compared to sham animals. TE, ES and TE+ES treatment following SCI markedly decreased $TRAP^+$ cells by −51.3%, −40.3% and −46.9%, respectively. Each intervention greatly reduced the ratio of RANKL to OPG mRNA of sublesional long bone. Collectively, our findings demonstrate that after neurologically complete paralysis, dynamic muscle resistance exercise by ES reduced muscle atrophy, downregulatd genes involved in muscle wasting, and restored mechanical loading to sublesional bone to a degree that allowed for the preservation of bone by inhibition of bone resorption and/or by facilitating bone formation.

Keywords

spinal cord injury; electrical stimulation; muscle; bone

Introduction

Immobilization results in muscle atrophy and decreased bone mass and structural integrity. Spinal cord injury (SCI) results in paresis or paralysis and protracted immobilization associated with extensive sublesional muscle atrophy and loss of bone mass and structural integrity [1–3]. In rats, bone loss following SCI develops rapidly, being evident within 2 days after complete spinal cord transection [4] and 2 weeks after a severe spinal cord contusion, and sublesional skeletal deterioration is most predominant for trabecular bone at the metaphasis and epiphysis of the femur and tibia where bone volume/total volume may be reduced by more than 50 percent [4–7]. Mechanisms implicated in bone loss in the period shortly after SCI are thought to primarily involve increased osteoclastic bone resorption with unchanged or slightly increased bone formation, apparently attributable to elevated cellular expression of receptor activator of NF-kB ligand (RANKL) and SOST, which encodes the protein sclerostin, a potent inhibitor of bone formation [5, 6, 8]. Loss of cortical bone has been reported in patients with SCI [2, 9], mice [10] and rats [7], although such loss occurs more slowly and to a lesser extent than that of trabecular bone, perhaps due to the smaller surface area accessible to osteoclasts for bone resorption.

Muscle atrophy following SCI is rapid, with muscle weights being reduced by 40 to 60% at two weeks after spinal cord transection when compared to sham-operated controls [11]. Mechanisms responsible are thought to involve primarily a marked upregulation of proteolytic degradation of muscle proteins likely attributable to the muscle-restricted E3 ubiquitin ligases muscle atrophy F-box (MAFBx, atrogin-1) and muscle ring finger-1 (MuRF1, Trim63), the expression of which is increased within days after SCI [1, 3, 11]. Both muscle atrophy and sublesional bone loss are mitigated in a dose-dependent manner by

testosterone [12]. Beneficial effects of testosterone on muscle atrophy have been reported to have numerous potential mechanisms of action that include suppression of MAFbx expression, upregulation of PGC-1α expression, activation of mTOR and suppression of FOXO activation [13–16]. In mice, androgen receptor knockouts reduce trabecular bone, apparently due to increased bone resorption [17]. Additionally, testosterone can undergo aromatization to estrogen which appears to be beneficial to preserving bone as demonstrated by findings deletion of the estrogen receptor alpha resulted in the reduction of trabecular bone [18].

An increase in physical activity, whether voluntary in the able-bodied or through use of surface or implantable electrical stimulation (ES) of nerves to elicit muscle contraction, has been shown to preserve muscle mass when initiated acutely after SCI, and restore, at least partially, muscle size and function once atrophy has occurred [19–21]. In rats with SCI, ES has been used to study acute responses of paralyzed muscle and bone to reloading [5, 22]. In those studies, ES was initiated approximately 4 months after SCI and continued for 7-days. While soleus muscles increased in weight in the SCI animals provided ES, expected changes in mitochondrial metabolism of carbohydrates and fats, and oxidative phosphorylation were not observed in contrast to controls in which muscle overloading by gastrocnemius ablation was conducted for the same period [22]. Cultured bone marrow progenitors were studied to understand how ES for 7 days may have influenced bone cells post-SCI [5]. Among the changes noted, numbers of osteoclast colonies, which increased in marrow from SCI animals, were decreased by ES, and, of interest, in cultures of marrow stromal cells under conditions favoring differentiation to osteoblasts, ES lowered SOST mRNA and raised mRNA for osteoprotegrin, a decoy receptor to RANKL, thus inhibiting the ability of RANKL to stimulate osteoclastogenesis and osteoclast activity [5]. However, no change in bone parameters was observed after 7 days of ES when assessed by microCT, most probably due to the short duration of ES. The purpose of this study was to determine the effects of an extended period of ES on muscle and bone in a rat model of severe SCI, and to test for synergist effects of ES when combined with supraphysiologic doses of testosterone.

Materials and Methods

Animals:

Animals: All animals were maintained on a 12:12-h light/dark cycle with lights on at 07:00 h in a temperature-controlled (20 ± 2°C) vivarium. All procedures were approved by the JJP VA Medical Center Institutional Animal Care and Use Committee and were performed in accordance with applicable requirements of NIH, PHS and VA.

Experimental Design: Animals were randomly assigned to either Sham SCI (laminectomy only) or SCI (spinal cord transection at T4). The SCI groups were randomly assigned to receive ES, testosterone enanthate (TE) or the combination. Interventions were initiated 2 weeks post surgery and continued for 4 weeks at which time tissue samples were collected for processing and animals were euthanized. The electrical stimulation for 4 weeks in this rat study is equivalent of approximately 2.5 years in humans (Ruth 1935) [23], representing a sufficient treatment duration when compared to months of intervention in

most clinical studies with electrical stimulation [24]. TE was administered intramuscularly to the quadriceps of the unstimulated right leg once a week at a dose of 4.0 mg; vehicle (sesame oil) was used in SCI or SCI+ES animals. Group sizes are as follows: Sham, n=13; SCI, n=13; SCI+TE, n=13; SCI+ES, n=10; and SCI+ES+TE, n=11.

ES Stimulators: ES was provided by implantable microstimulators with a single channel. Microstimulators were custom-designed and fabricated and encapsulated in silastic and gas sterilized. Stimulators were designed to be activated using a small magnet and had three modes of operation: off, testing and active. In the active mode, stimulators delivered 1.5 V at 40 Hz for 2 seconds followed by 18 seconds rest, as we described previously [5, 25]. Stimulation after severing the insertion of the gastrocnemius muscle into the Achilles tendon (see below for details) elicited some movement of the left foot and ankle with the ankle in a neutral position at approximately 90 degrees of dorsiflexion. Stimulation was provided for 60 min on each training day, five days a week.

Surgeries: Male Wistar rats (13 months old) underwent a complete spinal cord transection (T3–4) as previously described [4, 5, 22, 26–28]. Sham controls received laminectomy only at the same site, as previously described [5, 22]. Implantation of the stimulators was performed immediately after spinal transection, as previously described [5, 22], with some modifications. In brief, a small incision (~3 cm) was made over the left hip parallel to the femur. A pocket was created under the skin of the lower back for the stimulator. The pocket began at the point of origin of the incision with a size of approximately 5 by 5 cm. The bifurcation of the left sciatic nerve was exposed by blunt dissection. The stimulator was then inserted into the pocket and sutured in place with a single loop through a webbing tab; the two electrodes were tunneled subcutaneously from the back to the incision site over the bifurcation of the sciatic nerve. The first electrode was placed such that it nearly touched the anterior tibial nerve just cephalad to the nerve and about 0.8 cm distal to the bifurcation of the sciatic nerve. The second electrode was placed about 0.2 cm caudal from the common peroneal nerve at about 1 cm distal to the bifurcation. Tenotomy of the left gastrocnemius muscle was performed in all experimental groups by separating the tendons of the gastrocnemius, soleus and plantaris muscles and transecting the gastrocnemius muscle tendon. As demonstrated in our previous studies [5, 25], cutting the distal insertion of the gastrocnemius prevents concurrent contraction of this muscle from overwhelming the opposing force of the contracting tibialis anterior. SCI and Sham animals underwent an identical procedure except that no stimulator was implanted. We note that compared to our initial work with implanting the stimulators [5, 25], the size of the incision through which the electrodes are placed has been greatly reduced that was observed to considerably reduce excessive grooming and potential damage to the electrodes.

Fluorometric labeling of bone: Bones were labeled with fluorochromes by subcutaneous injection of calcein (10 mg/kg body weight) and xylenol orange (90 mg/kg body weight) on day −6 and day −2 before euthanasia, respectively [5, 26, 28].

ELISA assays

Serum C-terminal telopeptide of type I collagen (CTX) levels were measured using a RatLapsTM enzyme-immunoassay kit from Immunodiagnostic Systems (Fountain Hills, AZ). Serum concentrations of osteocalcin were measured using a rat osteocalcin immunoassay kit (Alfa Aesar). Serum levels of irisin were determined using a rat irisin competitive ELISA kit (Adipogen). All samples were assayed in duplicate, following the manufacturer's protocols.

Bone Density, Structure, and Strength

Areal bone mineral density (BMD) measurement was performed with a small animal dual energy X-ray absorptiometer (DXA) (Lunar Piximus, Fitchburg, WI, USA) as previously described [4, 6, 26, 27, 29, 30]. Volumetric BMD and bone architecture of the left distal femur and midshaft were assessed by a Scanco μCT scanner (μCT-40; Scanco Medical AG, Bassersdorf, Switzerland) at 21 mm isotropic voxel size as previously described [31, 32]. The μCT images were evaluated using standard software of the manufacturer to evaluate relative bone volume (BV/TV), trabecular number (Tb.N), trabecular thickness (Tb.Th), trabecular separation (Tb.Sp), structure model index (SMI), connectivity density (Conn.D), total cortical area (Ct.Ar), cortical thickness (Ct.Th), periosteal perimeter, and endosteal perimeter. Bone stiffness was estimated from micro finite element analysis (μFEA), following the manufacturer's recommended procedures, as previously described [4, 28, 33–37]. Briefly, μFEA models were produced by converting each bone voxel to an 8-node brick element. Bone tissue was computationally subjected to applied uniaxial compression, with an elastic modulus of 15 GPa and Poisson's ratio of 0.3 for each element. A linear elastic analysis was used to estimate the bone stiffness. Please see the Supplemental Materials and Methods for additional details.

Bone Histomorphometric Studies

For fluorochrome-based determination of rates of bone formation at the left distal femur by dynamic histomorphometry, 6 mm frozen sections embedded in methyl methacrylate plastic were cut using a Reichert-Jung sledge microtome. Xylenol orange and calcein were visualized by fluorescent microscopy and the distance between labeled layers was used as a measure of the rate of bone formation as determined by morphometry software. To quantify the osteoclast number and activity, tartrate-resistant acid phosphatase (TRAP) staining was used to specifically label osteoclasts in deplasticized distal femur sections. Slides were counterstained with hematoxylin and eosin (H&E). Osteoclasts were measured under bright field microscopy using an Olympus microscope with an OsteoMeasure system. Additional details regarding the procedures performed are provided in Supplemental Materials.

Extraction of total RNA from bone

Total bone RNA was extracted as previously described with some modifications [4, 38]. Briefly, long bones were dissected free of soft tissues, and bone marrow were flushed away with PBS using a 27G^{½} needle-syringe. The bone samples (~1g) were longitudinally cut into small piece and then digested 3 times with 2 mg/ml collagenase type I (Gibco, >150 Units; 20ml), one time with 5mM EDTA (Sigma-Aldrich,10 ml)), and one more with the

collagenase and EDTA, each for 25 min on a Shaker with rotation at 150 rpm at 37°C. Following the digestions, the bone samples were crushed using a mortar and pestle in liquid nitrogen. RNA was extracted from the lysate using the TRizol reagent (Sigma Aldrich) according to the manufacturer's instructions.

Ex vivo Osteoblastogenesis and Osteoclastogenesis Assay

Procedures for osteoblast and osteoclast formation from bone marrow stem cells were performed, as previously described [5, 27, 29–31, 39] and are described in greater detail in the Supplemental Materials.

RNA Extraction from Bone Marrow Cultures and Quantitative PCR

Total RNAs were extracted from bone marrow cell cultures using the TRI reagent (Sigma-Aldrich). One μg of total RNA was used to synthesize the first strand cDNA by the High Capacity cDNA Reverse Transcription Kit (Applied Biosystems). Real-time PCR determination of mRNA levels for specific mRNAs was determined with commercial primers from Taqman Assay On Demand probesets (Applied Biosystems) using the ViiA7 system (Applied Biosystems) as described previously [5, 27, 29–31, 39]. Relative expression levels were calculated using the $2^{-\Delta\Delta Ct}$ method with 18S RNA as an internal control [40]. Additional details regarding procedures performed are provided in Supplemental Materials.

Statistics

The mean values for study endpoints of stimulated (ipsilateral) left hindlimb among the experimental groups were compared. Data are expressed as mean ± standard error of the mean (SEM). The number of independent samples (n) is provided in the legend of each figure. The statistical significance of differences among means was tested using one-way analysis of variance and a Newman-Keuls post hoc test to determine the significance of differences between individual pairs of means using a p value of <0.05 to attain significance. Statistical calculations were performed using Prism 4.0c (GraphPad Software, La Jolla, CA, USA).

Results

Spinal cord transected animals lost approximately 10±3% percent of their preoperative body weight (Supplemental Fig. 1), a finding which is consistent with prior studies. Animals began gaining weight by day 10 post-injury and continued to gain weight until the end of the study at day 42 post injury (Supplemental Fig. 1). Implantation of a stimulator and / or administration of TE in SCI animals did not result in significant body weight change.

Beneficial Effects of ES and/or TE on Muscle:

To verify the effectiveness of ES in stimulating muscle overloading, weights of soleus, plantaris and extensor digitorum longus (EDL) muscles from hindlimbs were removed by careful dissection and weighed. The left (stimulated) muscles were evaluated and all muscle results are relative mass that has been corrected for body mass. As compared to sham-transected animals, significant reduction of the left soleus, plantaris and EDL muscle mass was found in animals that received complete spinal cord transection (Fig. 1A–C). Although

it did not reach statistical significance, TE, ES or the combination of these two treatments was linked to a numerical increase of the left (e.g., stimulated) plantaris muscle mass (+6.8%, +7.2% and +12.7%) and soleus muscle (+4.4%, +8.7% and +9.9%), respectively (Fig. 1A–B). Notably, ES alone or ES+TE treatment resulted in a clear and significant (~13%, $p<0.05$) increase of the left EDL muscle mass (Fig. 1C). Since SCI results in muscle atrophy and a shift of slow oxidative (e.g., soleus muscle) to fast glycolytic fibers (e.g., EDL muscle) [5, 41] and the observed changes on EDL muscle mass in response to ES alone or ES+TE treatment in this study (Fig. 1C), subsequent analyses will focus on the EDL muscle.

To further examine the effects of ES on muscle reloading, mRNA levels of two muscle atrophy related muscle-specific E3 ubiquitin ligases, MAFbx/atrogin-1 and Muscle RING Finger-1 (MuRF1) in the left EDL were examined. SCI resulted in a significant increase of MAFbx mRNA expression (Fig. 1D, $p<0.05$). TE injection did not change the MAFbx expression level, whereas a significant decrease of MAFbx mRNA was found upon ES alone or ES +TE treatment (Fig. 1D, $p<0.001$ and $p<0.05$, respectively). Of note, although no change of MurF1 mRNA expression was detected after SCI, each intervention, TE, ES or ES +TE, significantly reduced MurF1 mRNA levels (Fig. 1E, $p<0.05$, $p<0.01$ and $p<0.001$, respectively). The mRNA levels of the Wnt antagonists secreted frizzled-related protein (sFRP) 1 in the EDL muscle were increased after SCI, and were drastically reduced by TE injection, ES or ES+TE treatment (Fig. 1F, $p<0.001$). Compared to SCI animals, there was a non-significant trend of a decrease of sFRP2 after TE injection, but no change after ES or ES+TE (Fig. 1G).

Collectively, these data from sublesional skeletal muscle indicate that dynamic muscle resistance exercise by ES reduced muscle atrophy, downregulating key genes associated with muscle wasting. The alterations in muscle mass and total gene expression reflect biological changes as a direct consequence of ES intervention. The potential impact of mechanical reloading of muscle by ES on bone will be examined in subsequent studies.

Beneficial Effects of ES and/or TE on Bone Mass, Bone Structure and Bone Strength:

Dual energy x-ray absorptiometry (DXA) was performed using a small animal densitometer to determine bone mineral density (BMD) in rats after a complete spinal cord transection and TE injection, ES or TE+ES. At the left distal femur (Fig. 2A), BMD were decreased by −27% ($p<0.001$) after SCI, and significantly increased by +5.4% ($p=0.07$) and +8.5% ($p<0.01$) after ES and ES+TE treatments, respectively. An almost identical pattern of BMD change was also detected at the left proximal tibia (Fig. 2B) where BMD was reduced by −23.5% ($p<0.001$) after SCI. Compared to SCI, BMD at the proximal tibia increased +5.9% ($p<0.05$) and +11% ($p<0.001$) following ES and ES+TE treatment, respectively. The larger magnitude of changes on BMD in distal femur and proximal tibia in ES+TE animals as compared to TE or ES animals suggests a potential synergistic effect of TE and ES on bone mass. SCI also resulted in a −13.9% decrease of BMD at L3–5 (Fig. 2C). No effect of TE, ES or the combination was observed on BMD at L3–L5.

Bone architecture was examined by high-resolution μCT to access changes in trabecular bone at the distal femoral metaphysis (Fig. 3A). After SCI, trabecular bone volume (BV/TV) at this site was significantly reduced ($p < 0.001$, Fig. 3B), with decreased trabecular number

(Tb. N) (Fig. 3C), increased trabecular separation (Tb. Sp) (Fig. 3E) and no change in trabecular thickness (Tb. Th) (Fig. 3D). Trabecular connectivity (Conn. D) was greatly reduced (Fig. 3F), associated with transformation from plate-like to rod-like structures (Fig. 3G). Electrical stimulation alone or combined with TE significantly restored trabecular bone volume (Fig. 3B) by increasing trabecular number (Tb.N), which is associated with the increased connectivity (Fig. 3F) and the decreased value of the structure model index (SMI, Fig. 3G).

Cortical bone structure at the femoral midshaft was also examined by high-resolution μCT (Fig. 4A). SCI decreased cortical thickness (−9.0%, $p<0.05$, Fig. 4B). The decreased cortical thickness could be explained by a decreased periosteal perimeter (−7.0%, $p<0.05$, Fig. 4E) with no change on endosteal perimeter (Fig. 4F). Electrical stimulation in SCI animals partially restored periosteal perimeter (+4.9%, $p<0.05$, Fig. 4E). ES+TE administration completely restored cortical thickness (+9.5%, $p<0.05$, Fig. 4G), suggesting a synergistic effect of ES+TE.

Finite element analysis (FEA) based on μCT images was performed to predict the effect of ES and / or TE on bone mechanical property and strength. After SCI, midshaft bone stiffness estimated by FEA was reduced by −12.8% ($p<0.05$, Fig. 4F). ES alone or ES+TE led to a nearly complete restoration of cortical stiffness [+11.4% vs. SCI ($p<0.05$) and +12.8% vs. SCI ($p<0.01$), respectively, Fig. 4E].

Effects of ES and/or TE on Serum Levels of Bone Biomarkers and Bone Gene Expressions

ELISA assays were performed to examine the serum levels of bone biomarkers for formation, osteocalcin and resorption, CTX. Although no change of osteocalcin or CTX were detected following SCI, TE treatment alone or ES alone significantly increased the serum osteocalcin level ($p<0.05$ or $p<0.01$, respectively, Fig. 5A), while ES+TE treatment marginally decreased serum CTX level ($p=0.08$, Fig. 5B). Recent evidence showed that irisin, a myokine released after physical activitiy, increased cortical bone mass [42]. However, our ELISA assay showed that SCI did not change the serum irisin level, but ES alone, TE alone or ES+TE combined treatment after SCI all resulted in significantly reduced Irisin level compared to sham animals (Fig. 5C).

Total RNA from whole bone of hindlimb was extracted, and RANKL and OPG gene expression that are responsible for bone resorption and formation, respectively, was analyzed by quantitative PCR analysis. Following SCI, increases of the RANKL/OPG ratio ($p<0.01$, Fig. 5D) were observed in samples from SCI group compared with Sham-transected animals. The RANKL/OPG ratio was greatly reduced by ES or TE. The combination of ES +TE led to almost a complete normalization of RANKL/OPG ratio, approaching the ratio observed in Sham group (Fig. 5D).

Effects of ES and/or TE on Bone Formation and Bone Resorption

Dynamic histomorphometric analysis was performed to examine the effect of ES and/or TE on bone formation (Fig. 6A). Significant decreases in bone formation rate (BFR/TV, Fig. 6B), bone volume (BV/TV, Fig. 6F) and bone surface (B. Pm, Fig. 6G) were detected at the distal femur in animals with SCI. TE treatment significantly increased new bone formation

at the trabecular bone, as reflected by increases in the bone formation rate (BFR/TV, +110%, $p<0.05$, Fig. 6B), mineralizing surface (MS/BS, +22%, $p<0.05$, Fig. 6C), bone volume (BV/TV, +138%, $p<0.05$, Fig. 6F), bone surface (B. Pm, +109%, $p<0.05$, Fig. 6G), and dL Pm (+163%, $p<0.05$, Supplemental Fig 2B). ES significantly increased bone formation rate (Fig. 6B) and stimulated a trend for increases in mineral apposition rate (MAR, Fig. 6D), bone volume (Fig. 6F), and bone surface (Fig. 6G). ES tends to increase dL Pm (+36%, $p=0.06$, Supplemental Fig 2B) ES+TE treatment also partially restored single-labeled surface (sl.Pm) but not double-labeled surface (dl.Pm), both of which were decreased following SCI (Supplemental Figure 2A&B).

Sections of trabecular bone from the femoral metaphysis were immune-stained for TRAP (Fig. 7A). SCI resulted in trends for increases in both osteoclast surface (Fig. 7B) and osteoclast number (Fig. 7C). TE treatment alone or ES+TE treatments significantly decreased osteoclast surface and number (Fig. 7B–C), while ES alone only showed a trend for a decrease in osteoclast surface and number.

Effects of ES and/or TE on the Differentiation Potential of Bone Marrow Stem Cells

How ES and/or TE alter numbers of osteoclasts and osteoblasts in cultures of bone marrow cells was determined. The effects on bone cells of TE+ ES with the effects observed for ES or TE were compared. Osteoblastogenesis was evaluated by colony-forming unit-fibroblastic (CFU-F) staining using bone marrow mesenchymal stem cells derived from femurs from the left (e.g., stimulated) hindlimb (Fig. 8A). Consistent with our previous findings [5, 6, 27, 30], SCI decreased the numbers of CFU-F^+ cells by −56.8% ($p<0.05$) as compared to sham animals. Either TE or ES+TE treatment after SCI increased numbers of CFU-F^+ cells by +74.6% ($p<0.01$) and +67.2% ($p<0.05$), respectively, indicating greater potential of marrow stromal cells for osteoblastic differentiation. After SCI, decreased expression of Runx2 (Fig. 8C) and LRP5 (Fig. 8E) mRNA, as well as increased expression of SOST (Fig. 8D) and sFRP1 (Fig. 8F) mRNA were detected by quantitative PCR analysis. TE or ES+TE treatment significantly elevated the mRNA level of Runx2 and LRP5 (Fig. 8C, E); ES also increased the expression of these two osteoblastogenic markers but to a lesser extent. Interestingly, only ES+TE treatment decreased the expression of SOST and sFRP1 mRNA (Fig. 8D, F), suggesting a synergistic effect of ES in combination with TE to attenuate the expression of these markers for anti-anabolic action.

Consistent with our previous findings [5, 6, 27, 30], an osteoclastogenesis assay using bone marrow hematopoietic stem cells derived from the unstimulated femurs of SCI animals revealed a significant increase of +34.8% for $TRAP^+$ multinucleated cells ($p<0.001$) when compared to sham animals (Fig. 9B). Importantly, both TE treatment and TE-ES markedly decreased $TRAP^+$ cells by −51.3% ($p<0.001$) and −46.9% ($p<0.001$), respectively. Following SCI, quantitative PCR analysis revealed an increased expression in cultures of bone-marrow-derived osteoclasts of osteoclast marker genes including TRAP (Fig. 9C), integrin β3 (Fig. 9D) and calcitonin receptor (CTR, Fig. 9E). ES or ES+TE treatment significantly decreased the mRNA level of these three biomarkers for bone resorption, whereas TE treatment only decreased TRAP and CTR.

Discussion

The findings reported herein support several conclusions. Under the conditions of the experiment, ES and TE each improved some bone parameters (BMD at distal femur and proximal tibia, BV/TV by histomorphometry at the distal femur, BFR/TV by dynamic histomorphometry, and mechanical strength) and ES increased muscle mass, as might have been predicted from our prior studies in rats [22] and recent publications in persons with SCI [21]. While the combination of ES+TE caused numerical increases in BMD at these sites as compared to either treatment alone, there was no difference in BV/TV by microCT or histomorphometry between ES and ES+TE groups. Similarly, the combination of ES+TE did not increase muscle mass beyond that observed with ES alone. CFU-F^+ was reduced after SCI while numbers of $TRAP^+$ cells present in bone marrow cultures were increased after SCI. The pattern of changes in biochemical markers of osteoblast and osteoclast differentiation and activity generally paralleled the effects of ES and TE on bone mass. For example, ES and TE, alone or in combination, reduced numbers of $TRAP^+$ cells and osteoclast markers (TRAP mRNA and CTR mRNA). There was, however, some discordance between *ex-vivo* biological changes induced by ES alone or combined with TE as compared to effects of these interventions on bone parameters. For example, TE but not ES increased the number CFU-F^+ colonies; the pattern of effects of TE, ES or the combination on expression of Runx2 also suggested greater effects of TE as compared to ES, although criteria for statistical significance of differences between these groups were not met. When interpreting these discordant data, it should be appreciated that, while cell culture systems provide powerful tools that seem to recapitulate many important aspects of bone biology in disease, these cultures have limitations. Specifically, the process of isolation, fractionation and culture of cells may alter their biological properties when compared to their behavior *in vivo*.

Taken together, the data reported here do not demonstrate that restoring loading of bone by ES is synergistic with the bone-sparing activity of TE in a model of spinal cord transection performed in young adult rats. However, the findings do not exclude the possibility of synergy and there are trends in the data in which SOST and sFRP1 mRNA were lower in SCI+TE+ES (Fig. 8) while cortical bone outcomes of ES+TE were group higher (Fig. 4) relative to those in TE or ES alone groups, suggesting that a weak synergy could exist that could reach significance with larger sample size. The rather modest effect of ES on muscle mass was surprising given prior studies that demonstrated that the even small amounts of ES are sufficient to slow or prevent muscle atrophy after SCI in rats [19] or man [20]. In rats, muscle atrophy progresses rapidly after spinal cord transection; in a prior report, muscles from SCI animals were 40–60% smaller at 2 weeks compared with sham-transected controls [43]. Perhaps once atrophy is established, it is more difficult to reverse such atrophy by the application of ES. Alternatively, different ES paradigms from those used in the current study are required with respect to intensity, frequency or other parameters to restore, as opposed to prevent, post-SCI muscle atrophy. The skeleton of older animals is generally assumed to respond less to mechanical loading than that of younger animals; because 13-month old male rats were employed in the present study, it may have been anticipated that younger rats may have had a more robust response to ES. At present time, it is not known why treatment

with TE and/or ES induced more changes in the mass of EDL (mainly fast glycolytic muscle fibers) than in that of soleus (mainly slow oxidative muscle fibers) after SCI. Future study of muscle contractility, muscle fiber type and the associated molecular alterations can provide a better understanding of the changes observed in muscle function.

Androgenic steroids, including testosterone and nandrolone, have anabolic effects on bone [6]. Androgen ablation therapy for prostate cancer results in decreased bone mass [7]. In men treated chronically with glucocorticoids, testosterone increased lumbar spine BMD [8]. In women with osteoporosis, nandrolone increased BMD of the lumbar spine and femoral neck and reduced facture risk [9]. Recently, a number of publications from several groups, including ours, suggest that the reductions in circulating levels of testosterone, such as those that frequently occur in men after SCI [10, 11], may accelerate SCI-related bone loss [12] and also suggest that androgens may reduce such bone loss [13–15] , which perhaps is also the case in animals that are hypogonadal secondary to SCI [14]. Therefore, it is not surprising that although these rats with SCI had intact testes in the present study, testosterone administration has provided an anabolic effect on bone. Estrogen has an important role in muscle and bone physiology. As such, it would of interest to know if DHT, a form of testosterone which is not aromatizable, would have the same effects as the TE. Recent findings have demonstrated that DHT induced differentiation of a preosteoblast cell line in culture, and this action of DHT required Wnt signaling [16]. Similarly, our recent laboratory observation indicates that DHT inhibits expression of SOST mRNA (a key factor for controlling bone remodeling) in cultured osteocytic cells (data not shown). Therefore, we would expect that DHT would have a similar effect to that of TE on bone after SCI. TE was chosen as the hormonal intervention in the present study for several reasons. Testosterone replacement therapy is currently a therapy for older hypogonadal men [17] and for men who have loss of testosterone due to surgery [7]. Testosterone has been demonstrated to prevent loss of cancellous bone following SCI in a rat model [13–15], and it has shown a better safety profile on heart than DHT, although DHT can mimic most of the beneficial effects of testosterone.

Effects of ES on bone were more encouraging, and extend a prior report using similar stimulators, ES parameters and surgical models of SCI, including ablation of the insertion of the gastrocnemius into the Achilles tendon [5]. In that report, ES reduced numbers of TRAP + colonies in cultures of osteoclast precursors associated with downregulation of mRNA transcripts for osteoclast differentiation and activation genes, together with many favorable changes in mRNA levels in cultures of marrow stromal cells under osteoblastogenic conditions; these alterations included lower SOST and higher Wnt3a and osteoprotegrin mRNA levels. In the study reported here, four weeks of ES resulted in increases in multiple measures of metaphysial trabecular bone mass and higher BFR/TV while lowering osteoclast number in bone tissues and almost complete restoration of cortical mechanical strength, as predicted using FE modeling in the SCI animals at 6 weeks (a subacute phase of injury), suggesting a net anabolic effect on bone. Moreover, the mRNA ratio of RANKL to OPG in sublesional long bone was greatly reduced after the administration of ES, TE or ES +TE, suggesting that each intervention, or the combination, and the consequent reduction in bone resorption, at least in part, contributes to mitigate bone loss after SCI. One rather striking, and unexpected, finding is that osseous effects of ES appeared to be more

prominent than effects of ES on our muscle endpoints. Whether this reflects that the fact that bone loss progresses more slowly than muscle atrophy in this model system, such that bone is better able to respond to restoration of mechanical inputs, remains unclear.

As stated earlier, the reductions in circulating levels of testosterone, such as those that frequently occur in men after SCI [48, 49], may accelerate SCI-related bone loss [51] and also suggest that androgens may reduce such bone loss. In this study, we found that SCI+TE group had higher MS/BS and lower osteoclast numbers in bone sections, coincidental with more CFU-F^+ cells and higher Runx2 mRNA (meaning increased osteoblastogenesis) and lower $TRAP^+$ cells (meaning the reduced osteoclastogenesis) in bone marrow cell cultures, These changes are tightly associated with higher trabecular bone measures at distal femur. Our data confirm prior reports, including a recent study in which administration of TE spared bone and muscle following severe spinal cord contusion in rats [12], further suggesting the musculoskeletal benefits of TE administration. It should be noted that in the latter study, TE treatment was started immediately after SCI, rather than 2 weeks after injury as was performed in the current study. Thus, the smaller effect of TE on muscle and bone in the present study may to some degree relate to the timing of the delay in the initiation of treatment. For example, TE may be more effective in preventing muscle atrophy or bone resorption than its action to promote gains in muscle or bone mass once losses have occurred. It is interesting to note that TE suppressed MuRf1 and sFRP RNA in EDL and not MAFbx RNA. Future study will determine what it might imply about TE and how these factors may influence TE-mediated effects on muscle loss.

The myokine irisin is released from skeletal muscle upon exercise and contributes to certain favorable effects of physical activity. The roles of irisin in bone biology remains unsettled. Recent studies have demonstrated that administration of irisin can affect skeletal remodeling. For example, very low-dose irisin injections, administered intermittently, have been shown to improve cortical bone mineral density and strength in mice (Colaianni *et al.*, 2015, 2017; [2, 3]). These bone effects were consistent with *in vitro* studies showing that irisin could promote osteoblast differentiation (Qiao *et al.*, 2016; [4]). However, Bonewald's group and her collaborators recently reported that irisin increases sclerostin expression in osteocytes to induce bone resorption (Kim *et al.,* 2018; [5]). In the present study we observed that levels of irisin are decreased after each treatment performed, which is associated with a reduction in bone resorption and an increase in bone mass. This observation is consistent with the possibility that inhibition of irisin can reduce bone resorption and bone loss, whereas the induction of irisin can increase bone resorption and reduce bone mass, which appears to be in line with the studies by Kim *et al.* [5]. Similarly, there is lack of any consistent pattern observed with regard to changes of serum myostatin (another myokine) levels among the experimental groups (data not shown), which might be partially due to the generally appreciated cross-reactivity of myostatin with several members of the transforming growth factor beta (TGF-beta) family using commercial kits. Therefore, our present study is not able to state with any degree of confidence the role of either irisin or myostatin in the context of physical activity after SCI. Additional work is required to address the level and role of these two myokines or other soluble factors in improving our understanding of the ES-mediated beneficial effects on bone.

For future perspective, further study is needed to fully appreciate the potential of ES or ES-based combinatorial approaches to preserve or restore bone more chronically after SCI for an extended period of time with substantial sublesional bone loss, which represents the vast majority of the SCI population. Our initial analysis suggested the unexpected benefits on accrual of muscle and bone mass of the unstimulated (contralateral) right hindlimb that was observed in the absence of muscle contraction and bone reloading by ES (data not shown), leading to speculate that soluble factors that was released from muscle and/or bone upon ES-induced muscle contraction and bone reloading may be transported to the unstimulated hindlimb and, thereby, exert systemic musculoskeletal benefits. Future studies are warranted to further examine systemic alterations in bone homeostasis and remodeling and define the potential role of soluble mediators originating in skeletal muscle and/or bone that are responsible for humoral muscle-bone interactions in response to muscle contraction by ES. Additionally, the improvement of bone parameters in long bones (even contralateral long bones) but not the axial skeleton (L3–L5) is an important observation. It is unclear why the discrepancy was observed between the axial and appendicular skeleton, which remains a provocative topic to address in future investigation.

Supplementary Material

Refer to Web version on PubMed Central for supplementary material.

Acknowledgments

Sources of Research Support:

This work was supported by the Veterans Health Administration, Rehabilitation Research and Development Service (grants 5I01RX000687, 5I01RX001313 and 5I01RX02089-A2 to WQ; B9212-C and B2020-C to WAB), NIH R21 NS111393-01A1 to WQ, and the U.S. Department of Agriculture, Agricultural Research Service project plan #3062-51000-053-00D. USDA is an equal opportunity provider and employer. Mention of trade names or commercial products in this publication is solely for the purpose of providing specific information and does not imply recommendation or endorsement by the U.S. Department of Agriculture. The findings and conclusions in this manuscript are those of the authors and should not be construed to represent any official USDA of U.S. Government determination or policy.

References

1. Qin W, Bauman WA, and Cardozo C (2010). Bone and muscle loss after spinal cord injury: organ interactions. Ann N Y Acad Sci 1211 (1), 66–84. [PubMed: 21062296]
2. Bauman WA and Cardozo CP (2014). Osteoporosis in Individuals with Spinal Cord Injury. PM R.
3. Gorgey AS, Witt O, O'Brien L, Cardozo C, Chen Q, Lesnefsky EJ, and Graham ZA (2019). Mitochondrial health and muscle plasticity after spinal cord injury. Eur J Appl Physiol 119 (2), 315–331. [PubMed: 30539302]
4. Peng Y, Zhao W, Hu Y, Li F, Guo XE, Wang D, Bauman WA, and Qin W (2019). Rapid bone loss occurs as early as 2 days after complete spinal cord transection in young adult rats. Spinal Cord.
5. Qin W, Sun L, Cao J, Peng Y, Collier L, Wu Y, Creasey G, Li J, Qin Y, Jarvis J, Bauman WA, Zaidi M, and Cardozo C (2013). The Central Nervous System (CNS)-independent Anti-bone-resorptive Activity of Muscle Contraction and the Underlying Molecular and Cellular Signatures. J Biol Chem 288 (19), 13511–21. [PubMed: 23530032]
6. Qin W, Li X, Peng Y, Harlow LM, Ren Y, Wu Y, Li J, Qin Y, Sun J, Zheng S, Brown T, Feng JQ, Ke HZ, Bauman WA, and Cardozo CC (2015). Sclerostin antibody preserves the morphology and structure of osteocytes and blocks the severe skeletal deterioration after motor-complete spinal cord injury in rats. J Bone Miner Res.

7. Otzel DM, Conover CF, Ye F, Phillips EG, Bassett T, Wnek RD, Flores M, Catter A, Ghosh P, Balaez A, Petusevsky J, Chen C, Gao Y, Zhang Y, Jiron JM, Bose PK, Borst SE, Wronski TJ, Aguirre JI, and Yarrow JF (2019). Longitudinal Examination of Bone Loss in Male Rats After Moderate-Severe Contusion Spinal Cord Injury. Calcif Tissue Int 104 (1), 79–91. [PubMed: 30218117]
8. Jiang SD, Jiang LS, and Dai LY (2007). Changes in bone mass, bone structure, bone biomechanical properties, and bone metabolism after spinal cord injury: a 6-month longitudinal study in growing rats. Calcif Tissue Int 80 (3), 167–75. [PubMed: 17340221]
9. Eser P, Frotzler A, Zehnder Y, Wick L, Knecht H, Denoth J, and Schiessl H (2004). Relationship between the duration of paralysis and bone structure: a pQCT study of spinal cord injured individuals. Bone 34 (5), 869–80. [PubMed: 15121019]
10. Harlow L, Sahbani K, Nyman JS, Cardozo CP, Bauman WA, and Tawfeek HA (2017). Daily parathyroid hormone administration enhances bone turnover and preserves bone structure after severe immobilization-induced bone loss. Physiol Rep 5 (18).
11. Zeman RJ, Zhao J, Zhang Y, Zhao W, Wen X, Wu Y, Pan J, Bauman WA, and Cardozo C (2009). Differential skeletal muscle gene expression after upper or lower motor neuron transection. Pflugers Arch 458 (3), 525–35. [PubMed: 19214561]
12. Yarrow JF, Conover CF, Beggs LA, Beck DT, Otzel DM, Balaez A, Combs SM, Miller JR, Ye F, Aguirre JI, Neuville KG, Williams AA, Conrad BP, Gregory CM, Wronski TJ, Bose PK, and Borst SE (2013). Testosterone dose-dependently prevents bone and muscle loss in rodents following spinal cord injury. J Neurotrauma.
13. Zhao W, Pan J, Wang X, Wu Y, Bauman WA, and Cardozo CP (2008). Expression of the muscle atrophy factor muscle atrophy F-box is suppressed by testosterone. Endocrinology 149 (11), 5449–60. [PubMed: 18599544]
14. Zhao W, Pan J, Wang X, Wu Y, Bauman WA, and Cardozo CP (2008). Expression of the muscle arophy factor MAFbx is suppressed by testosterone. Endocrinology 149 (11), 5449–5460. [PubMed: 18599544]
15. Qin W, Pan J, Wu Y, Bauman WA, and Cardozo C (2010). Protection against dexamethasone-induced muscle atrophy is related to modulation by testosterone of FOXO1 and PGC-1alpha. Biochem Biophys Res Commun 403 (3–4), 473–8. [PubMed: 21094144]
16. Wu Y, Bauman WA, Blitzer RD, and Cardozo C (2010). Testosterone-induced hypertrophy of L6 myoblasts is dependent upon Erk and mTOR. Biochem Biophys Res Commun 400 (4), 679–83. [PubMed: 20816664]
17. Notini AJ, McManus JF, Moore A, Bouxsein M, Jimenez M, Chiu WS, Glatt V, Kream BE, Handelsman DJ, Morris HA, Zajac JD, and Davey RA (2007). Osteoblast deletion of exon 3 of the androgen receptor gene results in trabecular bone loss in adult male mice. J Bone Miner Res 22 (3), 347–56. [PubMed: 17147488]
18. Rooney AM and van der Meulen MCH (2017). Mouse models to evaluate the role of estrogen receptor alpha in skeletal maintenance and adaptation. Ann N Y Acad Sci 1410 (1), 85–92. [PubMed: 29148577]
19. Kim SJ, Roy RR, Kim JA, Zhong H, Haddad F, Baldwin KM, and Edgerton VR (2008). Gene expression during inactivity-induced muscle atrophy: effects of brief bouts of a forceful contraction countermeasure. J Appl Physiol (1985) 105 (4), 1246–54. [PubMed: 18653749]
20. Baldi JC, Jackson RD, Moraille R, and Mysiw WJ (1998). Muscle atrophy is prevented in patients with acute spinal cord injury using functional electrical stimulation. Spinal Cord 36 (7), 463–9. [PubMed: 9670381]
21. Gorgey AS, Khalil RE, Gill R, Gater DR, Lavis TD, Cardozo CP, and Adler RA (2019). Low-Dose Testosterone and Evoked Resistance Exercise after Spinal Cord Injury on Cardio-Metabolic Risk Factors: An Open-Label Randomized Clinical Trial. J Neurotrauma 36 (18), 2631–2645. [PubMed: 30794084]
22. Wu Y, Collier L, Qin W, Creasey G, Bauman WA, Jarvis J, and Cardozo C (2013). Electrical stimulation modulates Wnt signaling and regulates genes for the motor endplate and calcium binding in muscle of rats with spinal cord transection. BMC Neurosci 14 (1), 81. [PubMed: 23914941]

23. How old is a rat in human years? http://www.ratbehavior.org/RatYears.htm.
24. Martin R, Sadowsky C, Obst K, Meyer B, and McDonald J (2012). Functional electrical stimulation in spinal cord injury:: from theory to practice. Top Spinal Cord Inj Rehabil 18 (1), 28–33. [PubMed: 23459150]
25. Wu Y, Collier L, Qin W, Creasey G, Bauman WA, Jarvis J, and Cardozo C (2013). Electrical stimulation modulates Wnt signaling and regulates genes for the motor endplate and calcium binding in muscle of rats with spinal cord transection. BMC Neurosci 14 81. [PubMed: 23914941]
26. Qin W, Li X, Peng Y, Harlow LM, Ren Y, Wu Y, Li J, Qin Y, Sun J, Zheng S, Brown T, Feng JQ, Ke HZ, Bauman WA, and Cardozo CP (2016). Sclerostin Antibody Preserves the Morphology and Structure of Osteocytes and Blocks the Severe Skeletal Deterioration After Motor-Complete Spinal Cord Injury in Rats. J Bone Miner Res 31 (7), 1482. [PubMed: 27377772]
27. Sun L, Pan J, Peng Y, Wu Y, Li J, Liu X, Qin Y, Bauman WA, Cardozo C, Zaidi M, and Qin W (2013). Anabolic steroids reduce spinal cord injury-related bone loss in rats associated with increased Wnt signaling. J Spinal Cord Med 36 (6), 616–22. [PubMed: 24090150]
28. Zhao W, Li X, Peng Y, Qin Y, Pan J, Li J, Xu A, Ominsky MS, Cardozo C, Feng JQ, Ke HZ, Bauman WA, and Qin W (2018). Sclerostin Antibody Reverses the Severe Sublesional Bone Loss in Rats After Chronic Spinal Cord Injury. Calcif Tissue Int 103 (4), 443–454. [PubMed: 29931461]
29. Cardozo CP, Qin W, Peng Y, Liu X, Wu Y, Pan J, Bauman WA, Zaidi M, and Sun L (2010). Nandrolone slows hindlimb bone loss in a rat model of bone loss due to denervation. Ann N Y Acad Sci 1192 303–6. [PubMed: 20392251]
30. Bramlett HM, Dietrich WD, Marcillo A, Mawhinney LJ, Furones-Alonso O, Bregy A, Peng Y, Wu Y, Pan J, Wang J, Guo XE, Bauman WA, Cardozo C, and Qin W (2014). Effects of low intensity vibration on bone and muscle in rats with spinal cord injury. Osteoporos Int 25 (9), 2209–19. [PubMed: 24861907]
31. Qin W, Li X, Peng Y, Harlow LM, Ren Y, Wu Y, Li J, Qin Y, Sun J, Zheng S, Brown T, Feng JQ, Ke HZ, Bauman WA, and Cardozo CC (2015). Sclerostin antibody preserves the morphology and structure of osteocytes and blocks the severe skeletal deterioration after motor-complete spinal cord injury in rats. J Bone Miner Res 30 (11), 1994–2004. [PubMed: 25974843]
32. Bouxsein ML, Boyd SK, Christiansen BA, Guldberg RE, Jepsen KJ, and Muller R (2010). Guidelines for assessment of bone microstructure in rodents using microcomputed tomography. J Bone Miner Res 25 (7), 1468–86. [PubMed: 20533309]
33. Zysset PK, Dall'ara E, Varga P, and Pahr DH (2013). Finite element analysis for prediction of bone strength. Bonekey Rep 2 386. [PubMed: 24422106]
34. Lin T, Tong W, Chandra A, Hsu SY, Jia H, Zhu J, Tseng WJ, Levine MA, Zhang Y, Yan SG, Liu XS, Sun D, Young W, and Qin L (2015). A comprehensive study of long-term skeletal changes after spinal cord injury in adult rats. Bone Res 3 15028. [PubMed: 26528401]
35. Pistoia W, van Rietbergen B, Lochmuller EM, Lill CA, Eckstein F, and Ruegsegger P (2002). Estimation of distal radius failure load with micro-finite element analysis models based on three-dimensional peripheral quantitative computed tomography images. Bone 30 (6), 842–8. [PubMed: 12052451]
36. Lan S, Luo S, Huh BK, Chandra A, Altman AR, Qin L, and Liu XS (2013). 3D image registration is critical to ensure accurate detection of longitudinal changes in trabecular bone density, microstructure, and stiffness measurements in rat tibiae by in vivo microcomputed tomography (muCT). Bone 56 (1), 83–90. [PubMed: 23727434]
37. Liu XS, Zhang XH, Sekhon KK, Adams MF, McMahon DJ, Bilezikian JP, Shane E, and Guo XE (2010). High-resolution peripheral quantitative computed tomography can assess microstructural and mechanical properties of human distal tibial bone. J Bone Miner Res 25 (4), 746–56. [PubMed: 19775199]
38. Kitase Y, Vallejo JA, Gutheil W, Vemula H, Jahn K, Yi J, Zhou J, Brotto M, and Bonewald LF (2018). beta-aminoisobutyric Acid, l-BAIBA, Is a Muscle-Derived Osteocyte Survival Factor. Cell Rep 22 (6), 1531–1544. [PubMed: 29425508]

39. Qin W, Zhao W, Li X, Peng Y, Harlow LM, Li J, Qin Y, Pan J, Wu Y, Ran L, Ke HZ, Cardozo CP, and Bauman WA (2016). Mice with sclerostin gene deletion are resistant to the severe sublesional bone loss induced by spinal cord injury. Osteoporos Int.
40. Livak KJ and Schmittgen TD (2001). Analysis of relative gene expression data using real-time quantitative PCR and the 2(-Delta Delta C(T)) Method. Methods 25 (4), 402–8. [PubMed: 11846609]
41. Qin W, Bauman WA, and Cardozo C (2010). Bone and muscle loss after spinal cord injury: organ interactions. Ann N Y Acad Sci 1211 66–84. [PubMed: 21062296]
42. Colaianni G, Cuscito C, Mongelli T, Pignataro P, Buccoliero C, Liu P, Lu P, Sartini L, Di Comite M, Mori G, Di Benedetto A, Brunetti G, Yuen T, Sun L, Reseland JE, Colucci S, New MI, Zaidi M, Cinti S, and Grano M (2015). The myokine irisin increases cortical bone mass. Proc Natl Acad Sci U S A 112 (39), 12157–62. [PubMed: 26374841]
43. Zeman RJ, Bauman WA, Wen X, Ouyang N, Etlinger JD, and Cardozo CP (2009). Improved functional recovery with oxandrolone after spinal cord injury in rats. Neuroreport 20 (9), 864–8. [PubMed: 19424096]
44. Clarke BL and Khosla S (2009). Androgens and bone. Steroids 74 (3), 296–305. [PubMed: 18992761]
45. Schwandt A and Garcia JA (2009). Complications of androgen deprivation therapy in prostate cancer. Curr Opin Urol 19 (3), 322–6. [PubMed: 19318949]
46. Crawford BA, Liu PY, Kean MT, Bleasel JF, and Handelsman DJ (2003). Randomized placebo-controlled trial of androgen effects on muscle and bone in men requiring long-term systemic glucocorticoid treatment. J Clin Endocrinol Metab 88 (7), 3167–76. [PubMed: 12843161]
47. Frisoli A Jr., Chaves PH, Pinheiro MM, and Szejnfeld VL (2005). The effect of nandrolone decanoate on bone mineral density, muscle mass, and hemoglobin levels in elderly women with osteoporosis: a double-blind, randomized, placebo-controlled clinical trial. J Gerontol A Biol Sci Med Sci 60 (5), 648–53. [PubMed: 15972619]
48. Tsitouras PD, Zhong YG, Spungen AM, and Bauman WA (1995). Serum testosterone and growth hormone/insulin-like growth factor-I in adults with spinal cord injury. Horm Metab Res 27 (6), 287–92. [PubMed: 7557841]
49. Kostovski E, Iversen PO, Birkeland K, Torjesen PA, and Hjeltnes N (2008). Decreased levels of testosterone and gonadotrophins in men with long-standing tetraplegia. Spinal Cord 46 (8), 559–64. [PubMed: 18317482]
50. Bauman WA, La Fountaine MF, and Spungen AM (2014). Age-related prevalence of low testosterone in men with spinal cord injury. J Spinal Cord Med 37 (1), 32–9. [PubMed: 24090163]
51. Qin W, Bauman WA, and Cardozo CP (2010). Evolving concepts in neurogenic osteoporosis. Curr Osteoporos Rep 8 (4), 212–8. [PubMed: 20820963]
52. Beggs LA, Ye F, Ghosh P, Beck DT, Conover CF, Balaez A, Miller JR, Phillips EG, Zheng N, Williams AA, Aguirre JI, Wronski TJ, Bose PK, Borst SE, and Yarrow JF (2015). Sclerostin inhibition prevents spinal cord injury-induced cancellous bone loss. J Bone Miner Res 30 (4), 681–9. [PubMed: 25359699]
53. Yarrow JF, Conover CF, Beggs LA, Beck DT, Otzel DM, Balaez A, Combs SM, Miller JR, Ye F, Aguirre JI, Neuville KG, Williams AA, Conrad BP, Gregory CM, Wronski TJ, Bose PK, and Borst SE (2014). Testosterone dose dependently prevents bone and muscle loss in rodents after spinal cord injury. J Neurotrauma 31 (9), 834–45. [PubMed: 24378197]
54. Liu XH, Kirschenbaum A, Yao S, and Levine AC (2007). Androgens promote preosteoblast differentiation via activation of the canonical Wnt signaling pathway. Ann N Y Acad Sci 1116 423–31. [PubMed: 17646262]
55. Kenny AM, Kleppinger A, Annis K, Rathier M, Browner B, Judge JO, and McGee D (2010). Effects of transdermal testosterone on bone and muscle in older men with low bioavailable testosterone levels, low bone mass, and physical frailty. J Am Geriatr Soc 58 (6), 1134–43. [PubMed: 20722847]
56. Rubio-Gayosso I, Ramirez-Sanchez I, Ita-Islas I, Ortiz-Vilchis P, Gutierrez-Salmean G, Meaney A, Palma I, Olivares I, Garcia R, Meaney E, and Ceballos G (2013). Testosterone metabolites mediate

its effects on myocardial damage induced by ischemia/reperfusion in male Wistar rats. Steroids 78 (3), 362–9. [PubMed: 23276633]

57. Colaianni G, Mongelli T, Cuscito C, Pignataro P, Lippo L, Spiro G, Notarnicola A, Severi I, Passeri G, Mori G, Brunetti G, Moretti B, Tarantino U, Colucci SC, Reseland JE, Vettor R, Cinti S, and Grano M (2017). Irisin prevents and restores bone loss and muscle atrophy in hind-limb suspended mice. Sci Rep 7 (1), 2811. [PubMed: 28588307]
58. Qiao X, Nie Y, Ma Y, Chen Y, Cheng R, Yin W, Hu Y, Xu W, and Xu L (2016). Irisin promotes osteoblast proliferation and differentiation via activating the MAP kinase signaling pathways. Sci Rep 6 18732. [PubMed: 26738434]
59. Kim H, Wrann CD, Jedrychowski M, Vidoni S, Kitase Y, Nagano K, Zhou C, Chou J, Parkman VA, Novick SJ, Strutzenberg TS, Pascal BD, Le PT, Brooks DJ, Roche AM, Gerber KK, Mattheis L, Chen W, Tu H, Bouxsein ML, Griffin PR, Baron R, Rosen CJ, Bonewald LF, and Spiegelman BM (2018). Irisin Mediates Effects on Bone and Fat via alphaV Integrin Receptors. Cell 175 (7), 1756–1768 e17. [PubMed: 30550785]

Highlights

- Electrical stimulation (ES) or ES+ testosterone enanthate (TE) resulted in the increased mass of the EDL muscles in rats after Spinal cord injury (SCI).
- ES or ES+TE significantly decreased mRNA levels of muscle atrophy markers (e.g., MAFbx and MurF1) in the EDL.
- TE, ES and ES+TE treatment significantly increased trabecular bone mass at the distal femur.
- ES or ES+TE resulted in almost complete restoration of cortical stiffness in SCI animals.
- Dynamic muscle resistance exercise by ES reduced muscle atrophy and preserved bone by inhibition of bone resorption and/or by facilitating bone formation.

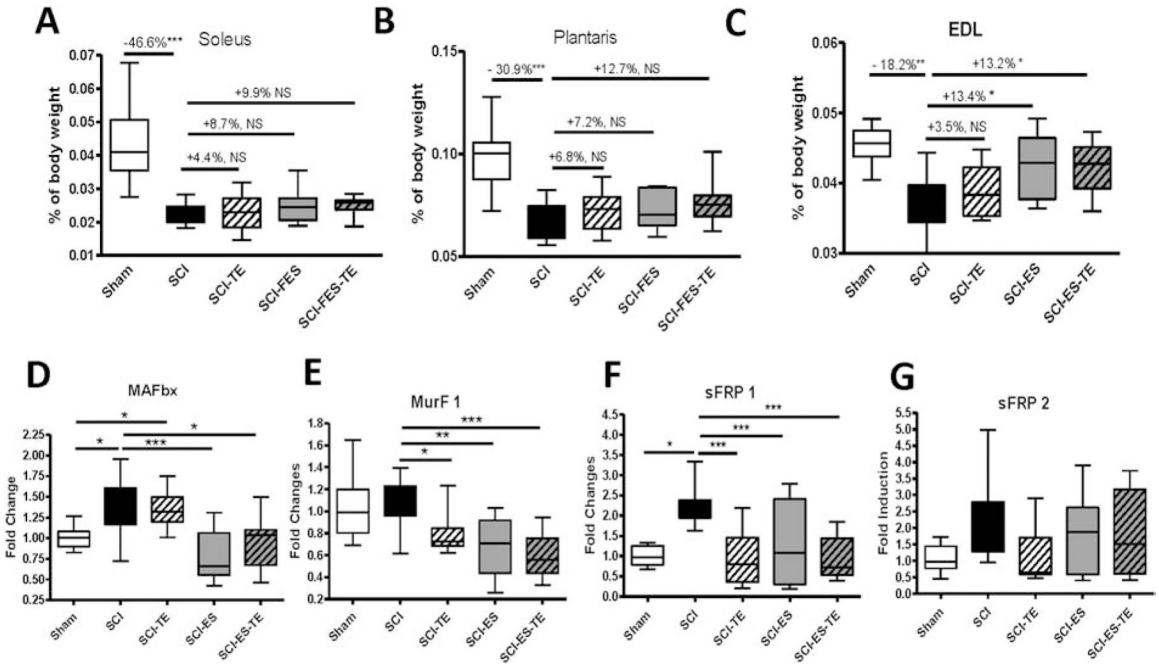

Figure 1. ES or ES+TE combination treatment reduced muscle loss after SCI.

(A–C) ES on muscle weight: **(**A) soleus muscle weight, (B) plantaris muscle weight, and (C) EDL muscle weight. (D–G) Effect of ES on the expression of muscle markers by measurement of changes in mRNA levels of EDL muscle genes by real-time PCR: (D) MAFbx, (E) MurF1, (F) sFRP1, and (G) sFRP2. Data are expressed as mean ± SE. N=10–13 per group. *p<0.05, **P<0.01, ***P<0.001 by one-way ANOVA.

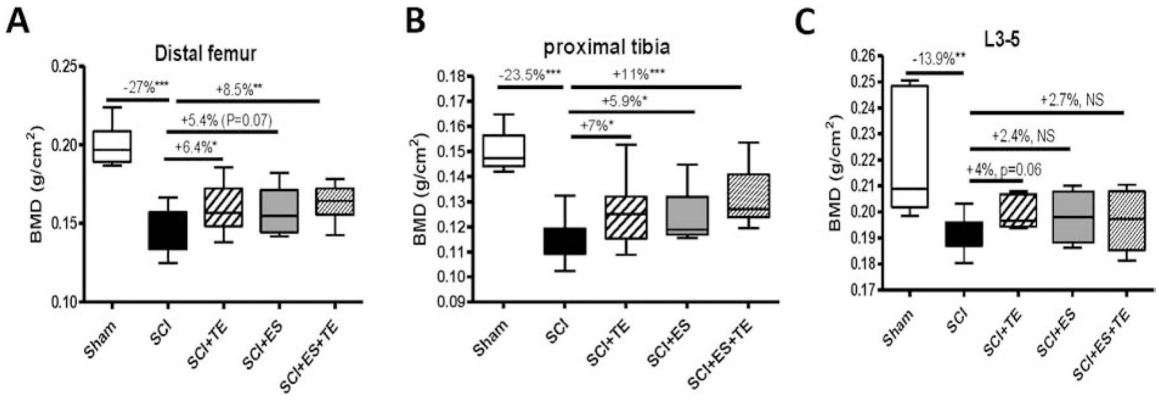

Figure 2. ES or ES+TE treatment reduced bone loss after SCI.

(A–C) Areal BMD measurements after complete spinal cord transection (T3–T4) at the: (A) distal femur, (B) proximal tibia, and (C) spine (L3–5). Sham-operated animals were used as controls. Data are expressed as mean ± SE. N = 10–13 per group. Significance of differences was determined using one-way analysis of variance with a Newman–Keuls post hoc test. *P < 0.05, **P < 0.01, ***P<0.001 versus the indicated group.

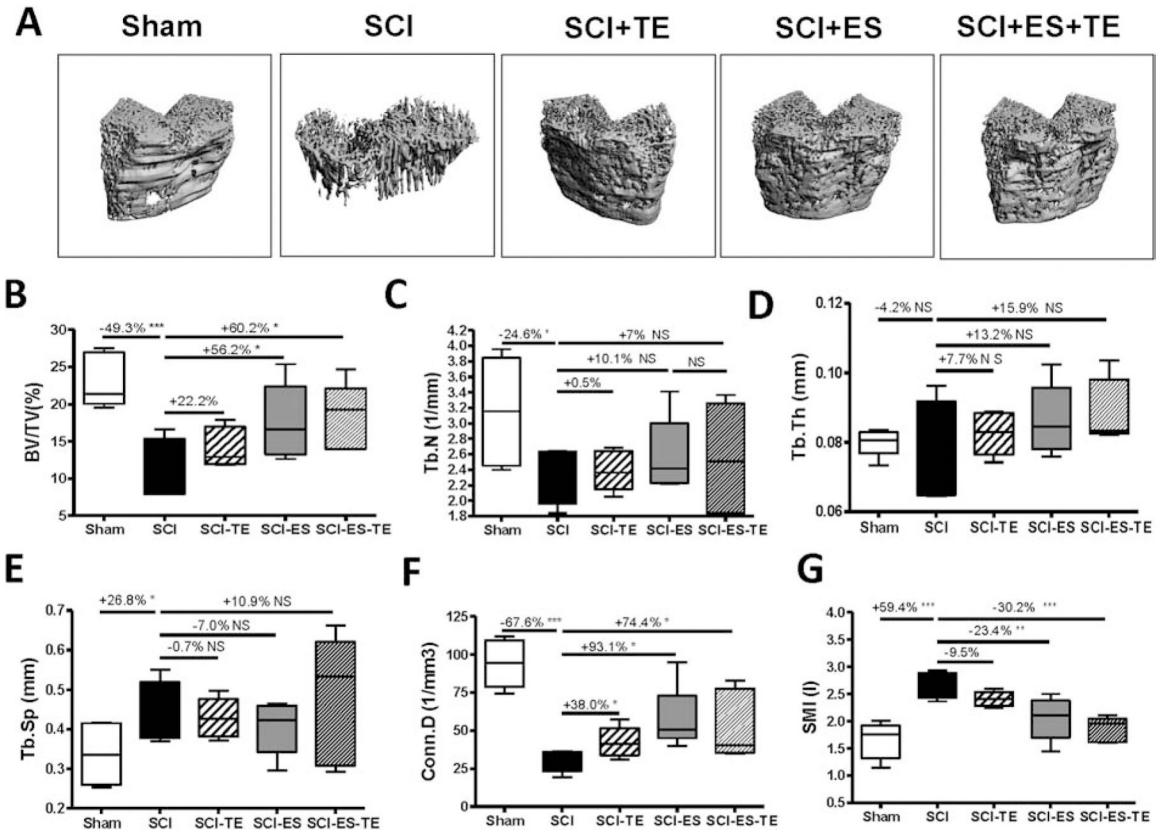

Figure 3. Effects of ES or ES+TE on trabecular architecture of the distal femur.

(A–F) Parameters of trabecular architecture: **(**A) representative μCT 3D images of trabecular microarchitecture; (B) trabecular bone volume per total volume (BV/TV%), (C) trabecular number (Tb.N), (D) trabecular thickness (Tb.Th), (E) trabecular space (Tb.Sp), (F) connectivity density (Conn.D), and (G) structure model index (SMI). Data are expressed as mean ± SE. N = 6 – 8 per group. Significance of differences was determined by using one-way ANOVA with a Newman–Keuls post hoc test. *P < 0.05, **P < 0.01 and ***P < 0.001 versus the indicated group.

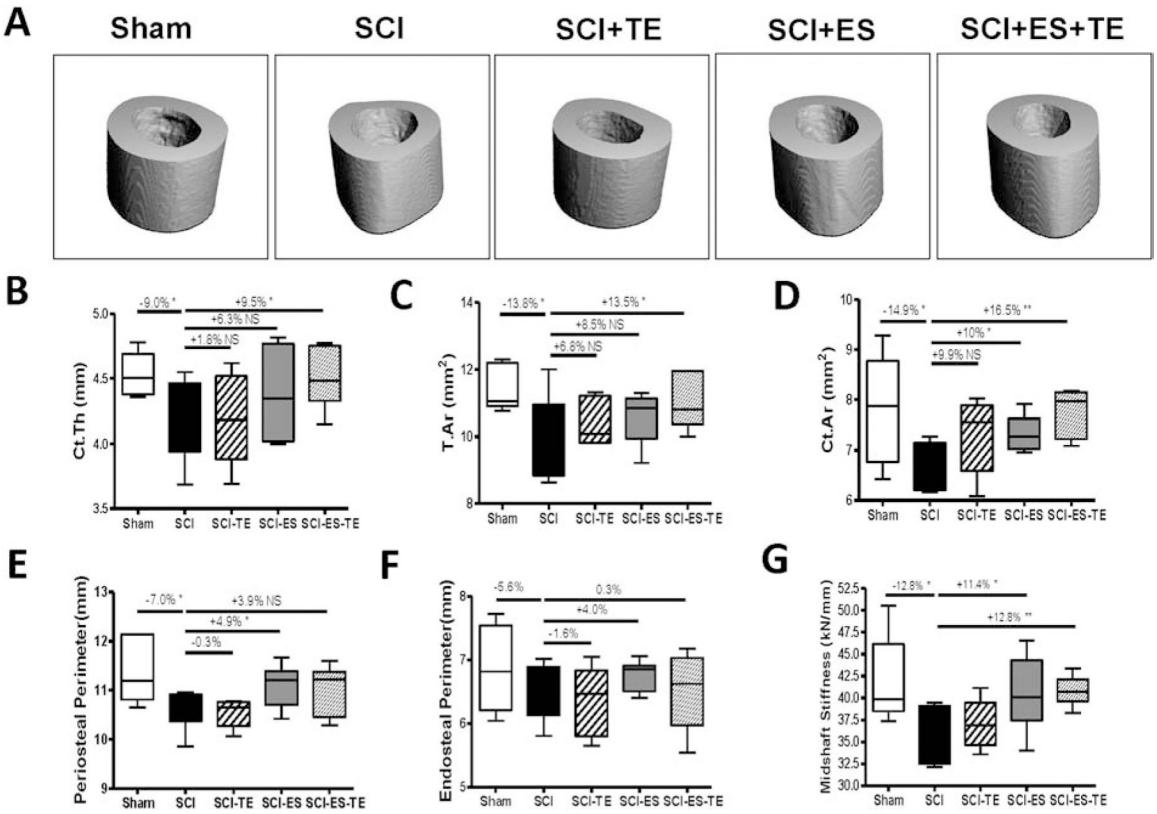

Figure 4. Effects of ES+TE on cortical architecture and strength of the femur midshaft.

(A–D) Parameters of cortical architecture: (A) representative μCT 3D images of cortical microarchitecture; (B) cortical thickness; (C) total tissue area; (D) cortical bone area; (E) periosteal perimeter, and (F) endosteal perimeter; Parameter of cortical strength: (G) stiffness. Data are expressed as mean ± SEM. N =6– 8 per group. Significance of differences was determined by using one-way ANOVA with Newman–Keuls post hoc test. *P < 0.05, ***P<0.001.

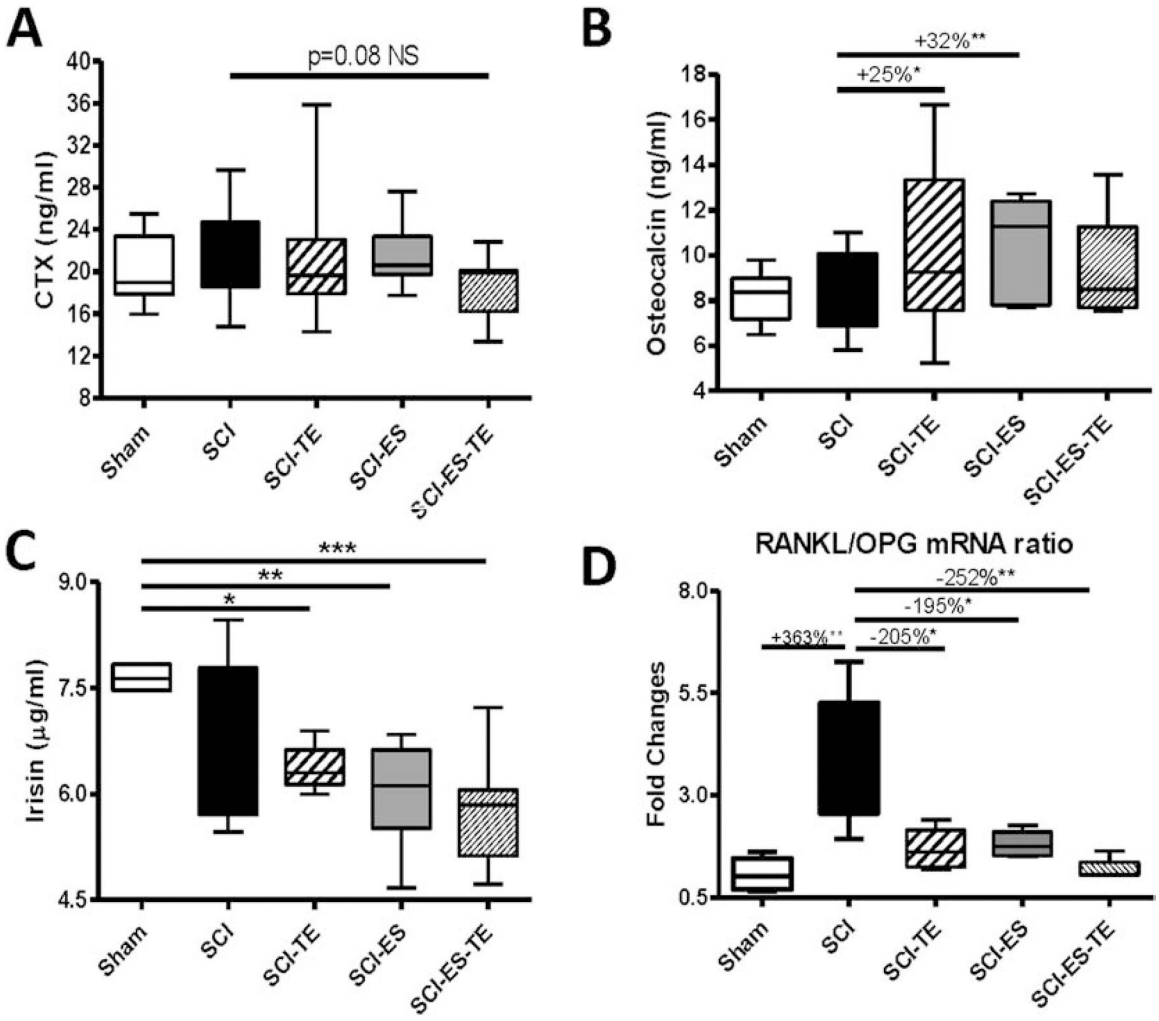

Figure 5. Effects of ES or ES+TE on levels of serum biomarkers of bone and RANKL/OPG mRNA ratio in long bone.

(A–C) ELISA tests for: (A) osteocalcin, (B) CTX, (C) irisin and (D) Using RNA extracted from sublesional long bones, RANKL and OPG gene expressions were determined by real-time PCR analysis and the ratio of RANKL/OPG was calculated. Data are expressed as mean ± SE, n=10–13 per group. *p<0.05, **p<0.01, ***p<0.001 by one-way ANOVA with Newman–Keuls post hoc test; #p<0.05, ##p<0.01 by two-tailed t-test.

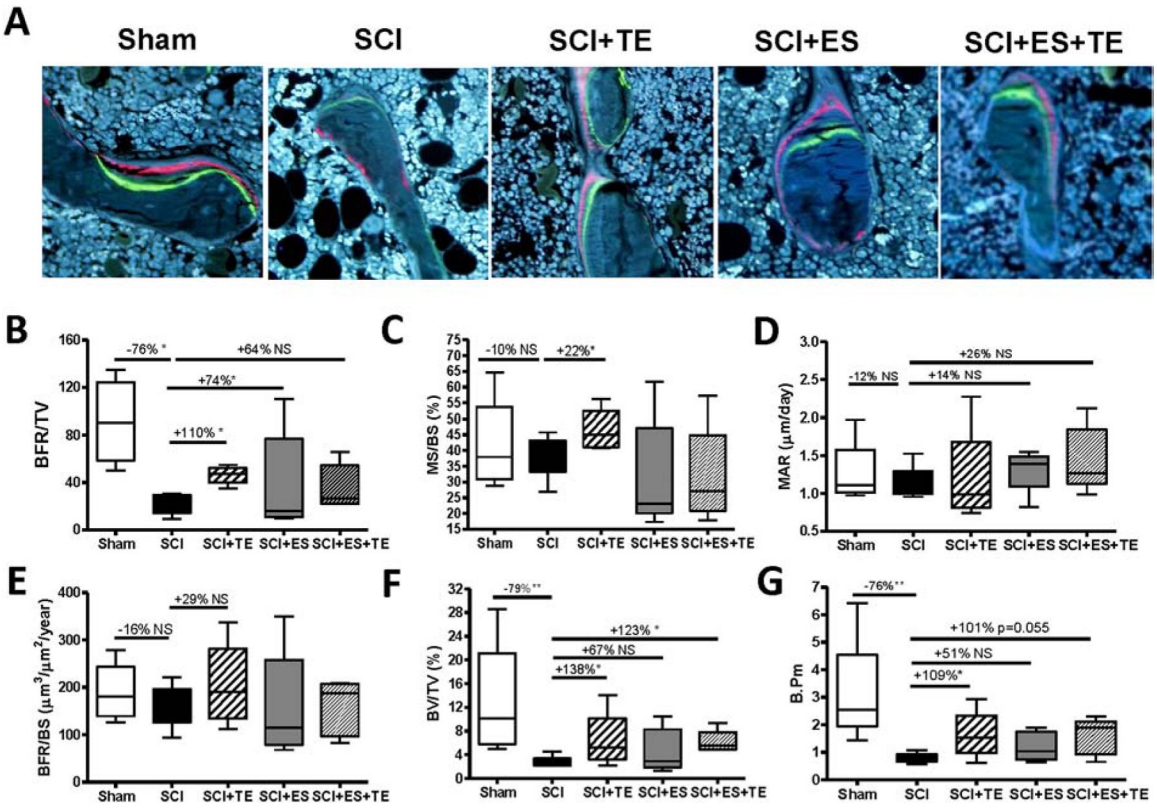

Figure 6. Effects of ES or ES+TE on formation of trabecular bone at the distal femur.

(A) Representative images of 6-μm-thick bone specimens showing double labeling of calcein and xylenol orange under fluorescence microscopy (magnification ×20). (B–G) Parameters of bone formation, volume and perimeter: (B) bone formation rate over tissue volume (BFR/TV), (C) mineralizing surface over bone surface (MS/BS), (D) mineral apposition rate (MAR), (E) bone formation rate over bone surface (BFR/BS), (F) bone volume over tissue volume (BV/TV), and (G) bone perimeter (B.pm). Data are expressed as mean ± SE, $^{**}p < 0.01$, $^{***}p < 0.001$ versus the indicated group by one-way ANOVA plus Newman–Keuls post hoc test, $n = 6–7$ animals per group.

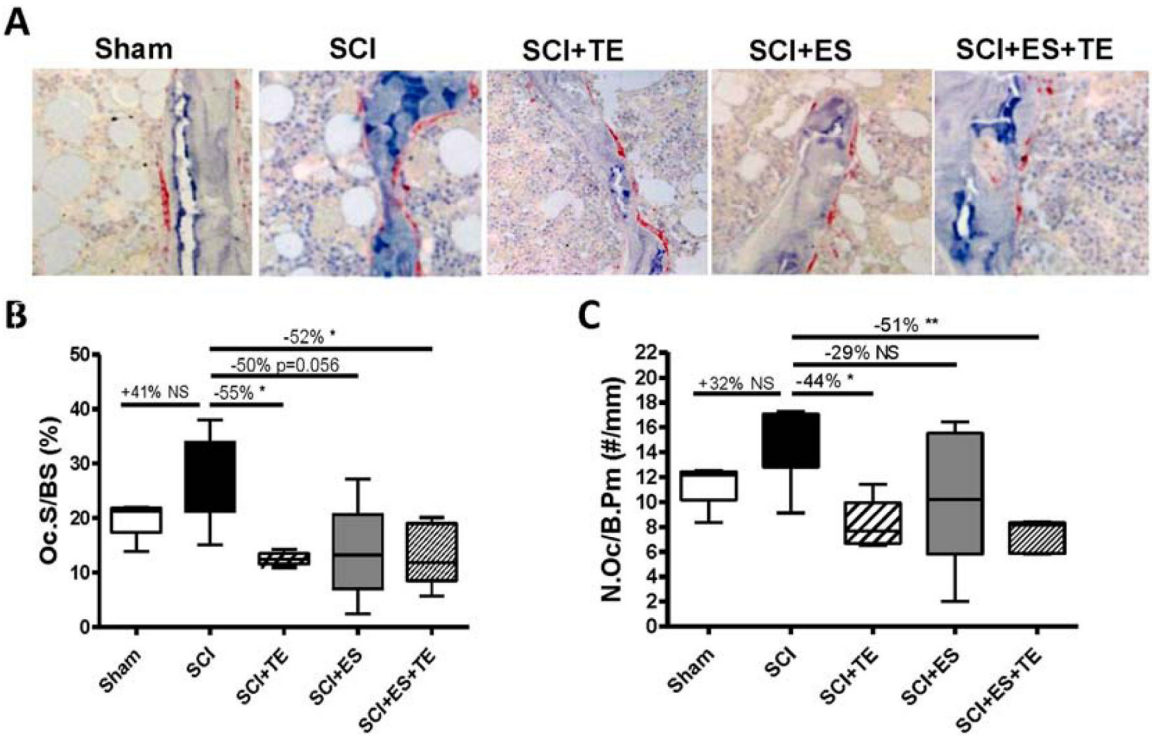

Figure 7. Effects of ES or ES+TE on bone resorption of trabecular bone at the distal femur.

(A) Representative sections of trabecular bone from the femoral metaphysis immunostained for TRAP (20x). The reddish areas of TRAP staining on trabecular surfaces representing osteoclasts. (B–C) Parameters of trabecular bone resorption by histomorphometric quantification: (B) osteoclast surface over bone surface (Oc.S/BS) and (C) osteoclast number over bone perimeter (N.Oc/B. Pm). Data are expressed as mean ± SE. N= 6–7 per group. *p<0.05 versus the indicated group by one-way ANOVA plus Newman–Keuls post hoc test.

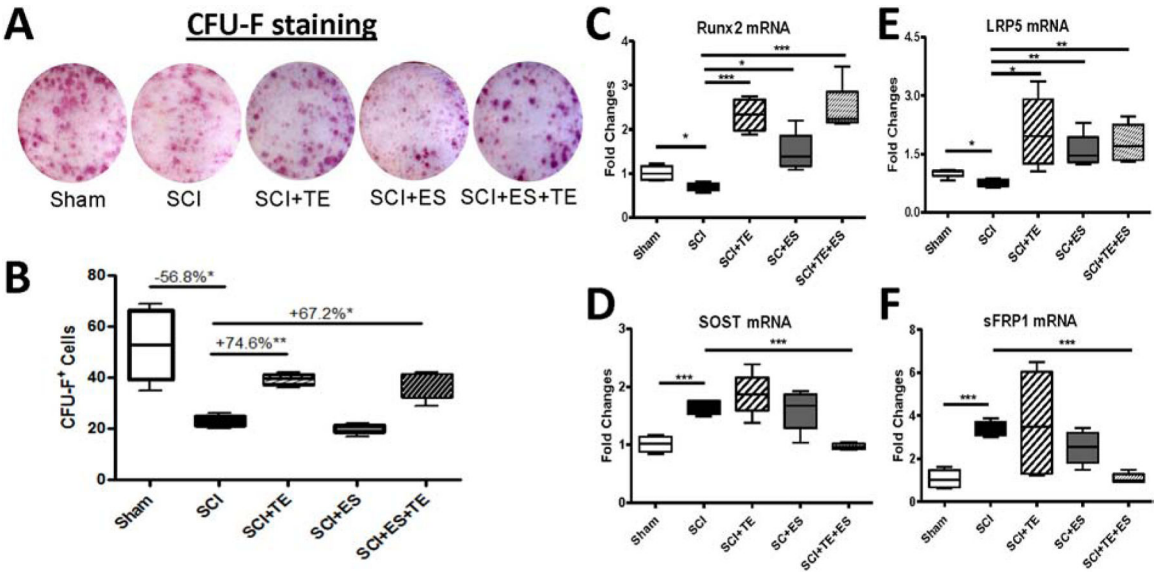

Figure 8. Effects of ES or ES+TE treatment on osteoblastic differentiation.

(A–B) Representative images of bone formation: (A) alkaline phosphatase staining (CFU-F) of cultured bone marrow stromal cells, and (B) quantification of CFU-F^{+} cells. (C–F) Changes in the gene expression of bone formation markers in cultured bone marrow stromal cells by quantitative PCR: (C) Runx2, (D) sclerostin (SOST), (E) LRP5, and (F) sFRP1. *p<0.05, ***p<0.001 by one-way ANOVA plus Newman–Keuls post hoc test, n=6–8 per group.

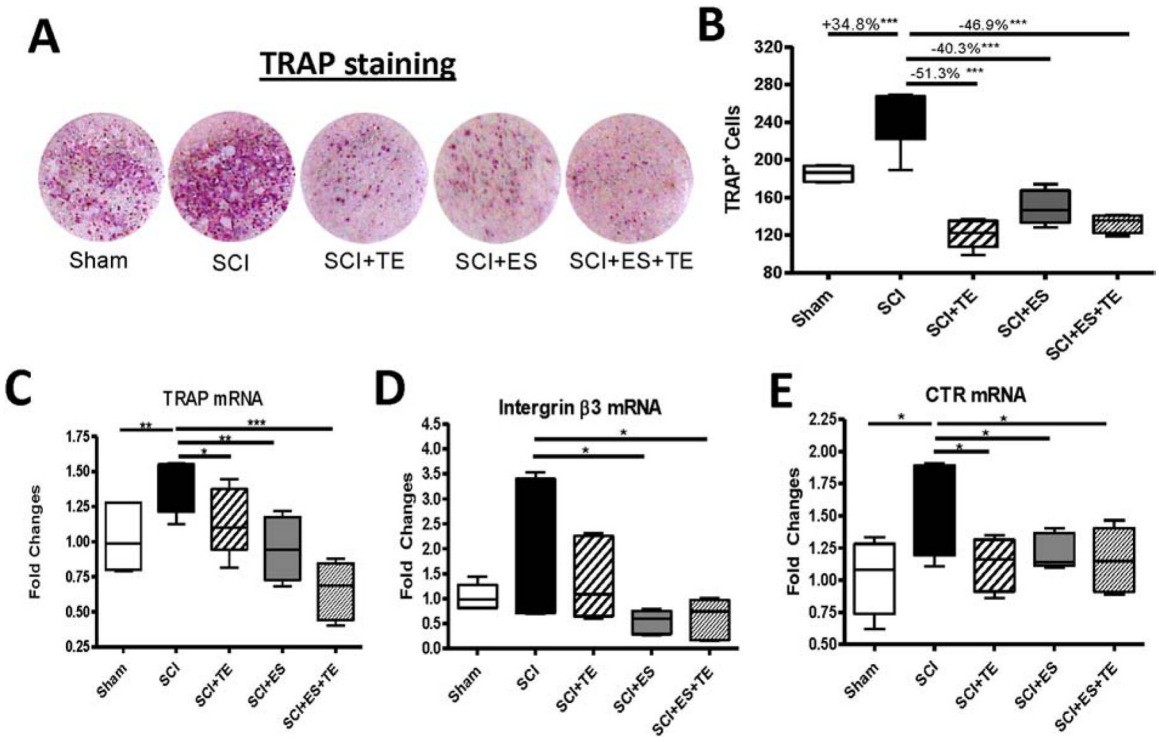

Figure 9. ES or ES+TE inhibited the osteoclastogenic potential of bone marrow hematopoietic cells.

(A) TRAP staining of cultured bone marrow hematopoietic cells, and (B) quantification of $TRAP^+$ cells. (C–E) Changes in the gene expression of bone resorption markers in cultured bone marrow hematopoietic cells determined by quantitative PCR: (C) TRAP, (D) integrin β3, and (E) calcitonin receptor (CTR). *p<0.05, **p<0.01, ***p<0.001 by one-way ANOVA plus Newman–Keuls post hoc test, n=6–8 per group.